Fabrication and Biocompatibility of Layer-by-layer Assembled Composite Graphene Oxide-polysaccharide Microcapsules

Svetozar Stoichev[1*], Avgustina Danailova[1], Ivan Iliev[1,2], Inna Sulikovska[2], Velichka Strijkova[1,3], Kirilka Mladenova[4], Tonya Andreeva[1]

[1]*Institute of Biophysics and Biomedical Engineering*
Bulgarian Academy of Sciences,
Acad. G. Bonchev Str., Bl. 21, 1113 Sofia, Bulgaria
E-mails: sd_stoichev@abv.bg, avgustina_danailova@abv.bg, t_andreeva@abv.bg

[2]*Institute of Experimental Morphology, Pathology and Anthropology with Museum*
Bulgarian Academy of Sciences
Acad. G. Bonchev Str., Bl. 25, 1113 Sofia, Bulgaria
E-mails: taparsky@abv.bg, inna_sulikovska@ukr.net

[3]*Institute of Optical Materials and Technologies*
Bulgarian Academy of Sciences
Acad. G. Bonchev Str., Bl. 109, 1113 Sofia, Bulgaria
E-mail: vily_strij@abv.bg

[4]*Faculty of Biology*
Sofia University "St. Kliment Ohriski"
8 Dragan Tsankov Blvd., 1164 Sofia, Bulgaria
E-mail: keti.mladenova@abv.bg

[*]*Corresponding author*

Received: July 21, 2021 **Accepted: February 17, 2022**

Published: September 30, 2022

Abstract: *The present study is focused on the construction and characterization of the morphology and biocompatibility of polysaccharide multilayered microcapsules (PMC) composed of natural polyelectrolytes (chitosan/alginate/hyaluronic acid), and on the effect of graphene oxide (GO) incorporation in the polymer matrix. The insertion of GO in the polymer matrix is an innovative and still evolving strategy used to modify the properties of the polyelectrolyte microcapsules. We have fabricated a number of hybrid GO-polysaccharide multilayered capsules by layer-by-layer assembling technique onto a $CaCO_3$ core, followed by core decomposition in mild conditions. Hybrid microcapsules with different composition were constructed by varying the number or localization of the incorporated GO-layers. It was found that the thickness of the hybrid microcapsules, evaluated by atomic force microscopy, decreases after incorporation of GO nanosheets in the polymer matrix. Analysis of the viability and proliferation of fibroblasts after incubation with hybrid PMC revealed pronounced concentration-dependent cytotoxic and antiproliferative effect. Based on the results, we can conclude that the hybrid multilayered microcapsules made of natural polysaccharides and graphene oxide could be used for biomedical applications.*

Keywords: *Graphene oxide, Polysaccharide microcapsules, Cytotoxicity, Antiproliferative activity.*

Introduction

Polyelectrolyte microcapsules (PEM) attract widespread interest as drug delivery platforms due to the possibility of fine optimization of their structural, mechanical and physicochemical. This improves the effectiveness in the functions they can perform, like site-specific drug delivery and drug protection, controlled sustained drug release, reducing adverse side effects and toxicity.

To date, a variety of approaches have been developed to model the properties of PEMs. The classical approaches based on adjustment of pH, ionic strength and temperature are non-invasive. Changes in pH and ionic strength induce an electro-osmotic shock that modulates the capsule's shell permeability, while high temperature leads to destabilization and dehydration of the polymer matrix [6, 8, 31]. The more advanced approaches include incorporation of non-polymer components in the polymer matrix and are more invasive. This is a widespread strategy for the formation of hybrid composite complexes between polyelectrolyte matrix of the capsules and various functional materials such as inorganic nanoparticles [2] carbon nanotubes [22], micelles [30], liposomes [27], biomolecules [19], and graphene derivatives [18].

In the recent years, the combination of carbon-based materials – carbon nanotubes, fullerenes and graphene oxide (GO) with a number of matrices have been widely used in biomedical and bioengineering technologies in the development of new materials for gene transfer, drug delivery, imaging, and tissue engineering. Particularly GO can easily form complex composite compounds with polymers [11, 14, 18, 23, 54]. Construction of various types of hybrid GO-polymer nanocomposite capsules composed of synthetic polyelectrolytes have been reported [28, 33, 46]. The presence of GO in the polymer matrix of multilayered GO/PAH (polyallylamine hydrochloride) capsules, built up by layer-by-layer (LbL) technology, renders unique properties, like permeability and dual capacity for "core-wall" encapsulation. However, studies on incorporation of GO into capsules made of biodegradable polymers with natural origin are still limited. Deng et al. [10] reported that the construction of hybrid polysaccharide multilayered capsules (PMC) with incorporated Fe_3O_4-functionalized GO makes them sensitive to external stimuli (magnetic field, infrared light). In other studies successful construction of GO-reinforced biodegradable microcapsules with good biocompatibility [29] and well-defined pH-controlled permeability over a wide pH-range [44] have been reported.

The problem with biocompatibility is fundamental regarding drug delivery systems [24]. The extent of biocompatibility of drug carriers depends on the fine balance between concentration and chemical structure of the carrier, the route of its administration as well as the contact time between drug carriers and live systems [20, 38, 51]. In the literature there is a lot of information about the dependence of the level of toxicity on the concentration of carriers with biodegradable nature [40]. Either of natural or synthetic origin, poly-cations have been shown to induce higher levels of cytotoxicity compared with poly-anions due to their stronger interactions with negatively charged cell membranes and subsequent cellular internalization [15, 21, 32, 49]. The microcapsules constructed of natural components can also inhibit the cell viability at higher values of the capsule to cell ratio. This can originate either to sedimentation of the capsules, which causes cells "stifling", or to mechanical damages of the cell membrane induced by the precipitated capsules [9, 42, 53].

Here we characterize the morphology and biocompatibility of PMC composed of biodegradable polyelectrolytes with natural origin (chitosan, alginate and hyaluronic acid) and

the effect of GO incorporation in the polymer matrix. We prepared a number of hybrid GO-polymer capsules (h-PMC) with different composition by varying the number of the deposited layers, as well as the number or localization of the GO-layers incorporated into the capsules' shell. The morphology (size, shape, surface roughness and thickness) of the capsules was evaluated by atomic force microscopy (AFM) and the PMC elasticity by nanoindentation. Additionally, the *in vitro* toxicity and antiproliferative activity on fibroblasts were evaluated at different capsules' concentration.

Materials and methods

Materials

Chitosan, Chi (MW 50-190 kDa, 75-85% deacetylated), fluorescein isothiocyanate conjugated bovine serum albumin (FITC-BSA), and ethylenediaminetetraacetic acid disodium salt (Na_2-EDTA) were purchased from Sigma-Aldrich (Germany). Sodium alginate, Alg (4-12 cP, 1% in H_2O, at 25°C) was purchased from Carl Roth & Co. (Karlsruhe, Germany). Sodium hyaluronate, HA (MW 130-300 kDa) was purchased from Contipro (Czech Republic). Graphene oxide (0.4 wt % water dispersion) from Graphenea (Spain). Calcium dichloride (dihydrate), disodium carbonate (anhydrous) and sodium chloride were analytical grade and used as received.

All solutions were made with ultra-pure water (18 MΩcm) in order to avoid influence of side ions. The polysaccharides were dissolved in 0.5 M NaCl to final concentration of 1 mg/mL. Before use, the GO dispersion was further diluted to 0.002 wt % (20 μg/mL) [10] with ultrapure water and ultrasonicated (30 min in ultrasonic bath, Iso Lab), in order to decrease the size of the GO-sheets. The pH of all working solutions was adjusted to 5.5 considering the pKa values of the functional groups of the structural elements used to build the capsules, so they were in ionized state.

Microcapsules preparation

Polysaccharide multilayer microcapsules were prepared onto freshly synthesized porous spherical calcium carbonate microparticles/cores (diameter range 4-10 μm) using standard centrifugation protocols [7, 10, 35, 37, 47] with some modifications. In brief, $CaCO_3$ cores were coated with oppositely charged polysaccharides, using LbL technique, by suspending the cores (approx. 2% w/v solid content) alternately in aqueous solutions of Chi, Alg or HA. The cores were incubated for 15 minutes in polysaccharide solutions and for an hour in GO suspension, at constant stirring at 600 rpm on magnetic stirrer (MS-H-Pro+, DLAB). After each deposition step, the coated cores were centrifuged (2 min at 200×g, Sigma 2-16 KL). Then the non-adsorbed polysaccharide chains or GO nanosheets were removed by double washing with 0.01 M NaCl after deposition of polysaccharides or with pure water after GO deposition, because NaCl screens the charges of the GO and lead to its aggregation [50]. After the construction of the target multilayer coating the coated $CaCO_3$ cores were dissolved by incubation in a solution of chelating agent – 0.02 M EDTA (pH 5.5). The resultant microcapsules were collected by centrifugation for 10 min (2500×g), then washed with ultrapure water and used immediately for analysis.

Optical microscopy

3D optical profiler, Zeta-20 (Zeta Instruments) was used for 3D imaging of the PMC and h-PMC. Zeta-20 enables imaging of surfaces with very low reflectivity and very high roughness. The equipment allows vertical (Z) resolution < 1 nm; field of view dimensions from 0.006 mm^2 to 15 mm^2; magnification from 5× to 100×; lateral resolution – sub-micron;

rapid data capture < 1 minute typical. The samples for optical microscopy were prepared by drop casting of the prepared capsule suspension in ultrapure water onto cleaned microscope glass slides and drying on air.

Scanning electron microscopy

Surface morphology of the composite capsules was determined by means of SEM (JEOL, JSM-7100F, Japan). Images were acquired at an average working distance of 9 mm with accelerating voltage of 10 kV. For SEM imaging the capsules were immobilized on glass slides by drop casting, dried and sputter-coated with 5 nm thin gold-layer to improve the conductivity of the surface and the quality of the acquired images.

Atomic force microscopy

Atomic Force Microscope (AFM) (Asylum Research MFP-3D, Oxford Instruments) was used supplied with silicon probes- qp-BioT (Nanosensors™) with a frequency of 20 kHz and a spring constant of 0.06 N/m. The experiments were carried out in contact mode with scan rate of 1 Hz. The samples were prepared by drop casting as for the optical microscope measurements.

Cell culturing

Biocompatibility of the different microcapsules formulations was evaluated on standard mouse embryonic BALB/3T3 fibroblasts. The fibroblasts were cultured in plastic flasks (Greiner, Germany) filled with medium mixture consisting of 90 % (v/v) Dulbecco Modified Eagle's medium (DMEM) (Gibco, Austria) and 10% (v/v) fetal bovine serum (Gibco, Austria). The culture medium was also supplemented with 100 U/mL penicillin (Lonza, Belgium) and 100 μg/mL streptomycin (Lonza, Belgium) under humidified air containing 5% CO_2 at 37°C.

In vitro biocompatibility assays

For the experiments with hollow microcapsules, the BALB/3T3 mouse fibroblasts suspended in culture medium (under a humidified 5% CO_2 atmosphere at 37°C) were seeded in the wells of a 96-well plate (Greiner, Germany) for 24 hours. For cytotoxic experiments the final cell number was in the order of 1×10^4 per well, while cell proliferation experiments were started with approximately 1×10^3 cells/well. The post seeding period allowed the cells to attach to the wells bottom.

The adhered cells were then treated with 200 μl of microcapsules suspensions with different concentrations (0.4, 0.8, 1.5, 3, 6, 12.5, 25 and 50%) and culture medium. The 50% PMC solution was prepared by mixing 100 μl of the initial microcapsules' suspension (approximately $12.8 \pm 0.8\times10^6$ capsules/mL, by naked-eye-counting on optical microscope images) with an equal volume of 100 μl culture medium, in order to avoid the risk of osmotic lysis of the cells. Untreated cells were used as controls.

The cell viability assay was performed 24 hours and the antiproliferative activity after 72 hours after incubation with microcapsules. Thereafter, microcapsules were removed and the number of viable/proliferated cells was evaluated by Neutral Red Uptake Assay [1, 41]. The cells were firstly treated with Neutral Red and then washed with methanol/acetic acid mixture and the extinction at 540 nm was measured on a TECAN microplate reader (TECAN, Grödig, Austria).

Statistical analysis

One-way ANOVA followed by Bonferroni's post hoc-test was used for statistical analysis. All experiments were done four times and data were presented as means ± standard deviation (SD). The lowest level of statistical significance was accepted ($p < 0.05$). Analysis was performed using SigmaPlot software.

Results and discussion

Characterization of PMC and h-PMC

Two main types of microcapsules without and with GO in the polymer matrix were prepared. Microcapsules without GO were referred as non-hybrid control polysaccharide multilayer microcapsules (cPMC), their shell composition is shown in Table 1. Four variants of h-PMC with GO included in their matrix have shell composition listed in Table 1.

Table 1. Shell composition of the studied PMC

Composition of the capsules' shell	Abbreviation
Chi/Alg/Chi/HA/Chi/HA	cPMC
GO/Chi/Alg/Chi/HA/Chi/HA	h-GO/P
Chi/Alg/Chi/GO/Chi/HA	h-P/GO/P
Chi/Alg/Chi/HA/Chi/GO	h-P/GO
Chi/Alg/Chi/GO/Chi/HA/Chi/GO	h-P/GO/P/GO

The efficiency of GO and PE deposition onto $CaCO_3$ cores was demonstrated by SEM imaging of the cores at the successive stages of the shell building (Fig. 1). The non-coated $CaCO_3$ cores have clear outlines and are well separated from each other (Fig. 1A), while the cores after 6 depositions cycles are coated with a thick polymer shell (Fig. 1D). Due to the intrinsic negative charge of the cores the poly-cation Chi was used in the 1st deposition step as a rule [17, 37, 47, 48] in the only exception is the h-GO/P variant where the LbL assembly was initiated with the deposition of a GO-layer. Sodium alginate has been used to enhance the strength of the polysaccharide matrix due to its capability to get rigid after crosslinking with divalent calcium cations from the dissolution of carbonate cores [13, 34, 39].

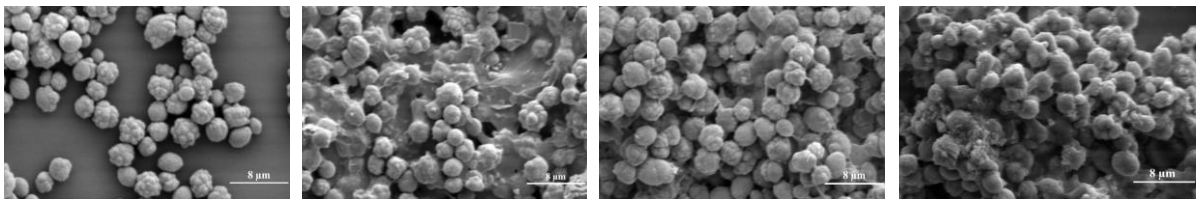

A) B) C) D)

Fig. 1 SEM images of $CaCO_3$ cores at different stages of capsule's shell build-up:
A) naked cores without shells; B) cores after deposition of a GO-layer;
C) after deposition of a Chi-layer;
D) core-shell microparticles with [Chi-Alg-Chi-HA-Chi-HA] shell.

Fig. 1B shows that after the incubation in aqueous GO dispersion $CaCO_3$ cores are wrapped by a thin shell. To confirm the successful deposition of GO on the cores, we measured the absorption of GO dispersion and the supernatant after centrifugation of the $CaCO_3$ cores incubated in GO suspension (Fig. 2). The typical absorbance maximum of GO at 230 nm is missing in the supernatant confirming GO nanosheets deposition on the $CaCO_3$ cores.

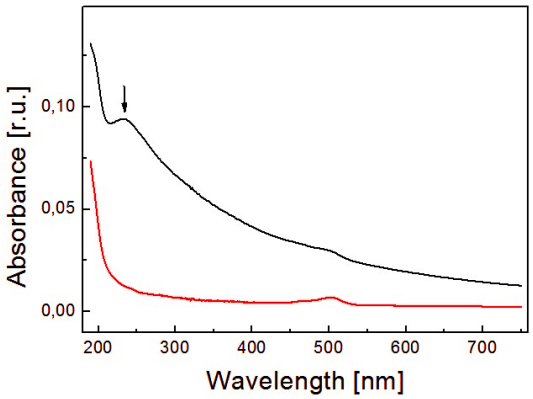

Fig. 2 Absorption spectra of GO suspension with concentration 20 µg/mL (black) and of the supernatant (red) after pelleting the $CaCO_3$ cores from the GO-$CaCO_3$ cores suspension. The arrow indicates the characteristic GO UV-band at 230 nm.

Moreover, the GO-$CaCO_3$ complexes did not dissociate even after several washings with pure water. All this indicates that despite the net negative charges at pH 5.5 of both graphene oxide (pKa of the carboxyl groups is < 3.75 [26] and the $CaCO_3$ cores, GO interacts stably with the calcium carbonate surface. The adsorption of GO on the surface of $CaCO_3$ cores was driven by the complexation of the surface exposed Ca^{2+} with the carboxyl and hydroxyl groups of GO [25].

Optical microscope images of the polysaccharide microcapsules obtained after dissolution of the $CaCO_3$ cores are presented in Fig. 3. The images show many polymorphic microcapsules, which is due to dehydration caused collapsing, shrinking and folding effects of the inherently soft polysaccharide shells. In addition, obvious heterogeneity for the h-P/GO/P/GO variant was observed (Fig. 3D).

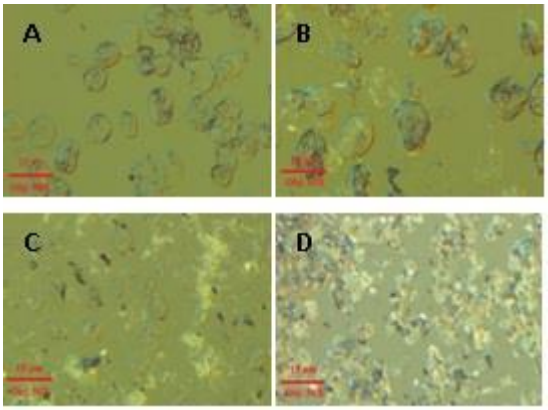

Fig. 3 Optical microscope images of dried hollow polysaccharide microcapsules: A) non-hybrid cPMC; B) hybrid h-GO/P; C) h-P/GO/P; D) h-P/GO/P/GO microcapsules.

High-magnification morphological images of collapsed capsules obtained by AFM are shown in Fig. 4 (micrographs of cPMC (A,B) and of h-P/GO/P/GO (D,E)). To determine the fine thickness of the polymer matrix cross-section profiles were made of the obtained micrographs. The thickness of the capsules was determined from the difference between the baseline and the lowest part of the capsule surface in order to avoid the influence of larger folds (Fig. 4C and F).

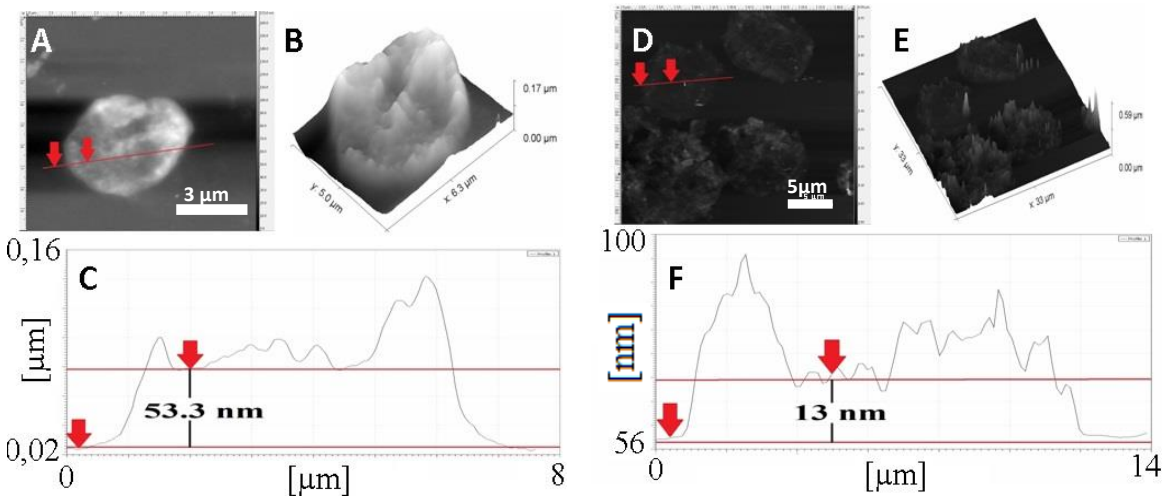

Fig. 4 Typical AFM micrographs of dried cPMC (A) and h-P/GO/P/GO (D) microcapsules, their corresponding three-dimensional presentations (B and E), and the cross-section profiles of image A (C), and of image D (F).

The mean doubled shell thickness of fully dried and collapsed non-hybrid cPMC, determined by AFM, was approximately 50 nm (49.1 ± 6.6 nm, Fig. 5), which corresponds to the doubled shell thickness of the capsules. All hybrid capsules appear thinner than the non-hybrid. The average thickness of all capsules with one GO-layer in the shell is practically the same within the measurement error (between 30-35 nm). Incorporation of one GO-layer decreases the doubled shell thickness by about 16 nm. Incorporation of second GO-layer decreases the thickness again by about 16 nm relative to the capsules with one GO-layer and it reaches 18.2 ± 5.2 nm for h-P/GO/P/GO capsules, which is about 2.7 times thinner than cPMC (Fig. 5).

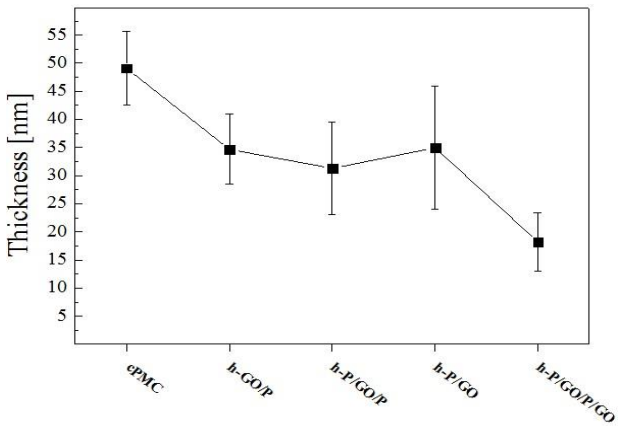

Fig. 5 Average doubled shell thicknesses of the different models of microcapsules

The significant reduction in the thickness is due to HA-layer replacement with GO-layer. In our previous study on hybrid PEM/GO films we demonstrated that the substitution of one HA-layer with GO-layer (1-2 nm thick) reduces the thickness by 5 to 7 nm [3]. Indeed, in contrast to the two-dimensional and atom-thick GO-sheets, the three-dimensional folded carbohydrate chains of HA can form complex diffuse scaffolds with the Chi-chains. It is not difficult to assume that the replacement of the large 3D hyaluronic molecules with 2D nanosized GO particles would lead to a significant thickness-reducing effect. It is also known that the electrostatic interactions between Chi and HA can be weak and unstable, due to the low charge density of the two natural polyions. It has been also shown that GO and Chi

can form stable nanocomposites with variety applications in biomedicine [11, 14, 23]. In case of h-GO/P capsules GO was deposited as 1st layer directly on the carbonate cores but not on the polymer matrix. The thinning effect in this case could be due to the presence of surface exposed GO nanolayer, which to some extent smoothes the porous and rough $CaCO_3$-surface and thus hinders the penetration of the polymers into the core matrix [29]. It has been shown that polymer bilayers deposited on porous carbonate particles are orders of magnitude thicker than the same layers built-up on a smooth substrate [47].

Biocompatibility assays

In this study 3T3 fibroblasts were exposed to series of dilutions of the different types of microcapsules (without and with GO), free GO nanosheets in a water suspension were used as controls. The highest concentration of GO nanosheets was equal to the concentration of GO suspension used in the deposition process (20 μg/mL).

The relative cellular viability and proliferation activity were determined for series of different capsules concentrations. The results were evaluated after 24 h for the cytotoxicity and after 72 h for the antiproliferative effect. The data are expressed as % relative to the negative control (untreated cells) (Fig. 6).

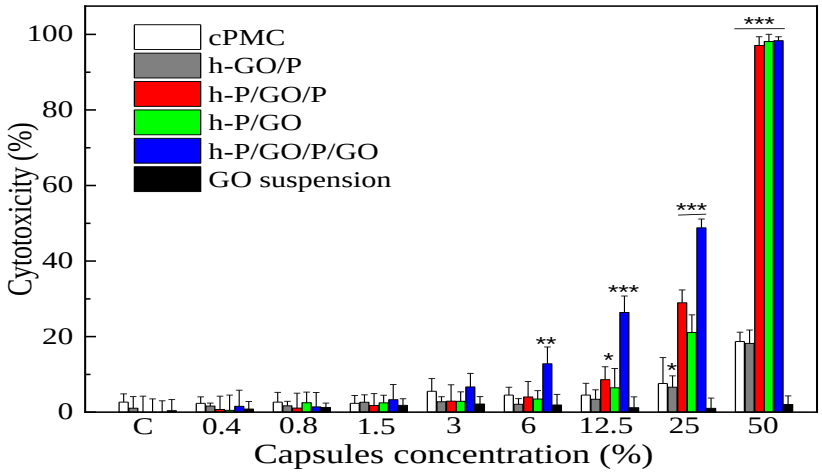

Fig. 6 Effect of capsules concentration on the *in vitro* cytotoxicity of BALB/3T3 mouse fibroblast cells after 24 h treatment. Cells cytotoxicity determined by 3T3 NRU test is expressed as percent of dead cells versus the negative control (C) presented as mean ± SD (n = 4), *** $p < 0.001$, ** $p < 0.01$, * $p < 0.5$, ANOVA test.

Correlation between the cytotoxicity and the microcapsules concentration was observed (Fig. 6) – all tested capsules reduce the cell viability in a concentration dependent manner. The non-hybrid cPMC and the hybrid h-PMC with one GO-layer (h-GO/P, h-P/GO/P and h-P/GO) show less than 10% cytotoxicity up to a concentration of 12.5% and there were no significant differences compared to the non-treated control cells. The cytotoxicity of h-P/GO/P/GO capsules with two GO-layers in the shell increases linearly with the concentration. cPMC without GO and h-GO/P capsules with one GO-layer located in the interior of the capsules show the same cytotoxicity which is lower than that of h-P/GO, h-P/GO/P and h-P/GO/P/GO capsules and does not exceed 20% non-survived cells even at the highest concentration studied. At 25% capsules suspension, with the exception of h-P/GO/P/GO capsules (50% non-survived cells), the rest of the capsules reached up to 25% non-survived cell only. All GO-containing capsules, except h-GO/P, show 100% cytotoxicity at the highest 50% concentration of the suspension. In comparison, cPMC and h-GO/P

capsules demonstrated much weaker cytotoxic effect – only 20% dead cells after treatment with the most concentrated (50%) capsule suspension. The suspension of free GO nanosheets did not show cytotoxicity at all.

Fig. 7 presents the cell viability (expressed in %) as a function of the concentration of both the tested capsules and of free GO nanosheets. Almost no differences were observed at low concentrations, while remarkable differences were found with the increase of the concentration and 3 groups of dependences can be distinguished. Group I included free GO-suspension, non-composite cPMC, as well as the composite h-GO/P capsules – all were almost non-toxic in the whole concentration range. The difference in the percentage of survived cells between the lowest (0.4%) and the highest (50%) capsules concentration was less than 20%. Group II (h-P/GO/P and h-P/GO) showed slight toxic effect at the low and average concentrations, but negative effect on the cells viability at the highest concentrations was quite obvious. The curves had rather an exponential pattern compared to Group I profiles – at the lowest capsule concentrations (from 0.4% to 12.5%) the number of non-survived cells was only 5% less than its corresponding value in Group I. At the average capsule concentrations (25%) this value increased up to 20%. However, it can still be seen that even at this concentration the capsules still do not show a pronounced cytotoxicity (over 70% survived cells). At the highest concentration (50%) approximately 100% of fibroblasts did not survive. The Group III included only h-P/GO/P/GO capsules characterized with the lowest biocompatibility compared to the other two groups – only 50% survived cells at 25% concentrated suspension (i.e., about 20% lower than the Group II values) (Fig. 7).

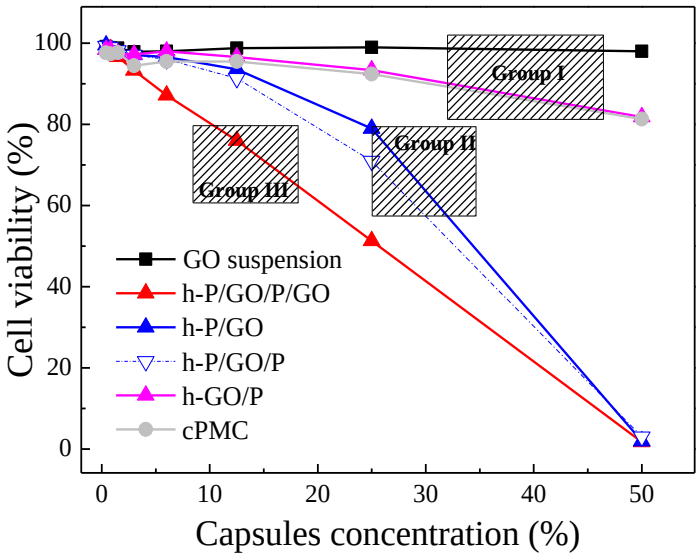

Fig. 7 Comparison of decreasing rates of *in vitro* cell viability
as function of capsules concentration. Data collection after 24 h treatment.

According to the data from Figs. 6 and 7, a quantitative estimation of the capsules' biocompatibility potential was determined, by calculation of the half from the maximum inhibitory capsules' concentration (IC_{50}). The data for the cytotoxicity and for antiproliferative effect are summarized in Table 2.

Based on the obtained results the most toxic h-P/GO/P/GO capsules reach IC_{50} at 25.59% capsules concentration which is with 7÷9% lower than the IC_{50}-values of Group II-capsules (with IC_{50} = 32÷34%). For the most non-toxic Group I-capsules, IC_{50} values were not reached even at 50% concentration of the capsules suspensions. On the other hand, the IC50 values for

antiproliferative activity are extremely low for all h-PMC samples – ranged between 3÷6% only. At the same time IC_{50} is significantly higher – 36.3% for the non-composite cPMC. This is clear indication that GO act as strong inhibitor of the 3T3 cells proliferation and this was also true for the h-GO/P capsules regardless of its lack of cytotoxicity. The hybrid capsules suppressed the cells proliferation much earlier than their cytotoxic activation. The IC_{50}-values for the GO-free suspension demonstrate lack of any cytotoxic or antiproliferative effect in the used concentration range (0.15÷20 μg/mL).

Table 2. Comparison of IC_{50} parameter between the different microcapsules formulations.

№	Samples	IC_{50} of mean ± SD (%)	
		Cytotoxicity	Antiproliferative activity
1	cPMC	> 50	36.33 ± 0.71
2	h-GO/P	> 50	3.33 ± 0.36
3	h-P/GO/P	32.69 ± 1.03	6.06 ± 1.14
4	h-P/GO	34.34 ± 0.84	6.69 ± 0.74
5	h-P/GO/P/GO	25.59 ± 1.14	6.07 ± 0.56
6	GO suspension	> 50	> 50

Note: IC_{50} values were calculated after 24 h (for the cytotoxicity) and after 72 h (for the antirpoliferative activity) treatment with microcapsules

The significant discrepancies in the biocompatibility of the capsules demonstrated in Fig. 6, Fig. 7 and Table 2 might result from the capsules' stiffness. The physicochemical properties of nano- and microparticles (such as size, shape, surface chemistry, stiffness and elasticity) have been found to exert significant effects on the cellular internalization pathways [16, 45]. A model study also showed that the stiffer capsules required less adhesion energy to binding the cell membrane than softer ones [52]. Based on the fact that GO-layers exhibit extremely high stiffness (Young's modulus ~ 200 GPa [43] and that incorporation of GO increases the stiffness of the soft polyelectrolyte multilayer films [5, 36] we suppose that the PMC become stiffer after GO incorporation. Hence, we classified the investigated here capsules as softer (cPMC and h-GO/P) and stiffer (h-P/GO, h-P/GO/P and h-P/GO/P/GO). We classify h-GO/P-caps as softer because GO does not affect the capsule shell stiffness, but rather fills the capsular lumen after the decomposition of $CaCO_3$ cores. Furthermore, we have already demonstrated a strong dependence of the surface stiffness of HA/Chi multilayer films on both the position and the abundance of GO-layers in the polymer matrix [3].

However, the effect of the protocol of GO-deposition during microcapsules preparation – i.e., GO was deposition below (h-GO/P capsules) or above (h-P/GO/P, h-P/GO and h-P/GO/P/GO capsules) the alginate layer cannot be excluded. It is possible that the GO nanosheets destabilize the weakly interacting Chi and HA and therefore amorphous GO-Chi and GO-Chi-HA complexes might be formed that can create a large area for harmful contact with cell membranes. Regarding the h-GO/P capsules, the alginate layer may act as a barrier that prevents GO nanosheets to destroy the outer Chi/HA layers.

The different decreasing rates in Fig. 7 as well as the discrepancies in IC_{50} values (Table 2) can be explained by the complementary influence of the capsules concentration, the stiffness of the capsules shell and the polydispersity of the capsules suspensions. Monodisperse suspensions of softer cPMC and h-GO/P capsules exhibit the weakest adhesion with the cell membranes and cytotoxicity correlates only with the capsule concentration. The IC_{50} was not

reached even at the highest incubation concentrations (IC_{50} > 50%, Table 2). As a result, a slight slope of the curves of viability vs. capsules concentration was observed (Fig. 7, Group I). However, regarding the h-P/GO and h-P/GO/P capsules, the inhibitory effect of the capsules concentrations was further combined with the both – increased capsule stiffness and higher extent of polydispersity. As a consequence, the stronger adhesion and sedimentation on the underlying cells led to a pronounced cell inhibitory effect at lower capsules concentrations (IC50 ~ 32÷34%, Table 2) and to a more pronounced exponential decrease of the viability (Fig. 7, Group II). The inhibitory effect of h-P/GO/P/GO capsules was most evident (IC_{50} = 25.6%) due to the additional GO-layer and the high degree of polydispersity (Fig. 3D). The pronounced inhibitory effects induced by h-P/GO/P, h-P/GO and h-P/GO/P/GO were probably due to significant capsules sedimentations causing cells stifling as well as some membrane injures. Taking into account the initial number of microcapsules in the none-diluted suspension and the number of treated cells per well (see *In vitro biocompatibility assays* section), it was easy to define the rude capsules to cell ratio. The most concentrated (50%) samples contained approx. 6.4×10^6 microcapsules, which means caps/cell = 128/1. So that, our results are consistent with the observations by other researchers that at ~ 12/1 ratio (i.e., the 3÷6% capsules suspensions), no cytotoxicity was observed, regardless of the microcapsule variants [10].

The lack of any inhibitory effect of free GO nanosheets can be due to lack of sedimentation over the cells for the following reasons: (i) the negatively charged GO nanoparticles were electrostatically repulsed by the negatively charged cell membranes and (ii) at low concentrations used in this study (0.15÷20 μg/mL) the free GO nanosheets formed a stable and uniformly dispersed suspension. In addition, our results are consistent with previous reports proving that free GO suspension is not cytotoxic at concentrations up to 50÷75 μg/mL [12, 14].

Conclusion

It was demonstrated that the incorporation of GO into the polymer shell of polysaccharide-based microcapsules strongly reduced the capsules' thickness. Analysis of the viability and proliferation of fibroblast cells after treatment with hybrid microcapsules revealed pronounced concentration-depending cytotoxic and antiproliferative effects. The localization of GO-sheets in the polymer shell determines the degree of cytotoxicity of the microcapsules – those with the deepest deposited GO layer have the lowest cytotoxic effect comparable with the non-hybrid capsules.

This study showed the possibility of fine-tuning the properties of polysaccharide microcapsules by refining the protocol for the deposition of GO in the capsule matrix that can serve as a fundamental basis for the more precise design of biodegradable microcapsules.

Acknowledgements

This work was supported by grant КП-06-M21/4, Competition for financial support for basic research projects of young scientists and postdoctoral fellows – 2018, Bulgarian National Science Fund. Research equipment of Distributed Research Infrastructure INFRAMAT, part of Bulgarian National Roadmap for Research Infrastructures, supported by Bulgarian Ministry of Education and Science was used in this investigation.

References

1. 3T3 Neutral Red Uptake (NRU) Phototoxicity Assay, Invittox Protocol No. 78, http://ecvam-dbalm.jrc.ec.europa.eu
2. Anandhakumar S., S. P. Vijayalakshmi, G. Jagadeesh, A. M. Raichur (2011). Silver Nanoparticle Synthesis Novel Route Laser Triggering Polyelectrolyte Capsules, ACS Appl Mater Interfaces, 3(9), 3419-3424.
3. Andreeva T., A. Dér, L. Kelemen, R. Krastev, S. Taneva (2020). Modulation of the Internal Structure and Surface Properties of Natural and Synthetic Polymer Matrices by Graphene Oxide Doping, Polymers for Advanced Technologies, 31(7), 1562-1570.
4. Andreeva T., S. Stoichev, S. Taneva, R. Krastev (2018). Hybrid Graphene Oxide/Polysaccharide Nanocomposites with Controllable Surface Properties and Biocompatibility, Carbohydrate Polymers, 181, 78-85.
5. Andreeva T., H. Hartmann, S. Taneva, R. Krastev (2016). Regulation of the Growth, Morphology, Mechanical Properties and Biocompatibility of Natural Polysaccharide-Based Multilayers by Hofmeister Anions, J Materials Chemistry B, 4(44), 7092-7100.
6. Antipov A. A., G. B. Sukhorukov, S. Leporatti, I. L. Radtchenko, et al. (2002). Polyelectrolyte Multilayer Capsule Permeability Control, Colloids Surf. A: Physicochem Eng Asp, 198-200, 535-541.
7. Antipov A., D. Shchukin, Y. Fedutik, A. I. Petrov, et al. (2003). Carbonate Microparticles for Hollow Polyelectrolyte Capsules Fabrication, Colloids Surf. A: Physicochemical and Engineering Aspects, 224(1-3), 175-183.
8. Burke S. E., C. J. Barrett (2004). pH-dependent Loading and Release Behavior of Small Hydrophilic Molecules in Weak Polyelectrolyte Multilayer Films, Macromolecules, 37(14), 5375-5384.
9. De Koker S., B. G. De Geest, C. Cuvelier, et al. (2007). *In vivo* Cellular Uptake, Degradation, and Biocompatibility of Polyelectrolyte Microcapsules, Adv Funct Mater, 17(18), 3754-3763.
10. Deng L., Q. Li, S. Al-Rehili, H. Omar, et al. (2016). Hybrid Iron Oxide-graphene Oxide Polysaccharides Microcapsule: A Micro-matryoshka for Ondemand Drug Release and Antitumor Therapy *in vivo*, Appl Mater Interfaces, 8(11), 6859-6868.
11. Duan J., F. Liu, Y. Kong, M. Hao, et al. (2020). Homogeneous Chitosan/Graphene Oxide Nanocomposite Hydrogel Based Actuator Driven by Efficient Photothermally Induced Water Gradients, ACS Appl Nano Mater, 3(2), 1002-1009.
12. Ege D., A. Kamali, A. R. Boccaccini (2017). Graphene Oxide/Polymer-based Biomaterials, Adv Eng Mater, 19(12), 16-34.
13. Fathy M., S. M. Safwat, S. M. El-Shanawany, S. S. Tous, M. Otagiri (1998). Preparation and Evaluation of Beads Made of Different Calcium Alginate Compositions for Oral Sustained Release of Tiaramide, Pharm Dev Technol, 3(3), 355-364.
14. Figueroa T., C. Aguayo, K. Fernandez (2020). Design and Characterization of Chitosan-Graphene Oxide Nanocomposites for the Delivery of Proanthocyanidins, Int J of Nanomedicine, 15, 1229-1238.
15. Fischer D., Y. X. Li, B. Ahlemeyer, J. Krieglstein, T. Kissel (2003). *In vitro* Cytotoxicity Testing of Polycations: Influence of Polymer Structure on Cell Viability and Hemolysis, Biomaterials, 24(7), 1121-1131.
16. Gratton S., P. Ropp, P. Pohlhaus, J. Luft, et al. (2008). The Effect of Particle Design on Cellular Internalization Pathways, PNAS, 105(33), 11613-11618.
17. Gupta G. K., J. Vikas, P. R. Mishra (2011). Templated Ultrathin Polyelectrolyte Microreservoir for Delivery of Bovine Serum Albumin: Fabrication and Performance Evaluation, AAPS Pharm Sci Tech, 12(1), 344-353.

18. Hong J., K. Char, B.-S. Kim (2010). Hollow Capsules of Reduced Graphene Oxide Nanosheets Assembled on a Sacrificial Colloidal Particle, Phys Chem Lett, 1(24), 3442-3445.
19. Hosta-Rigau L., S. F. Chung, A. Postma, R. Chandrawati, et al. (2011). Capsosomer with "Free-floating" Liposomal Subcompartments, Adv Mater, 23(35), 4082-4087.
20. Huang M., E. Khor, L.-Y. Lim (2004). Uptake and Cytotoxicity of Chitosan Molecules and Nanoparticles: Effects of Molecular Weight and Degree of Deacetylation, Pharmaceudical Research, 21(2), 344-353.
21. Hunter A. C. (2006). Molecular Hurdles in Polyfectin Design and Mechanistic Background to Polycation Induced Cytotoxicity, Adv Drug Deliv Rev, 58(14), 1523-1531.
22. Ji L., M. Jin, C. Zhao, W. Wei, et al. (2006). Porous Hollow Carbon Nanotube Composite Cages, Chem Commun, 11, 1206-1208.
23. Justin R., B. Chen (2014). Characterisation and Drug Release Performance of Biodegradable Chitosan-graphene Oxide Nanocomposites, Carbohyd polym, 103, 70-80.
24. Kohane D. S., R. Langer (2010). Biocompatibility and Drug Delivery Systems, Chem Sci, 1(4), 441-446.
25. Kondoh A., T. Oi (1998). Interaction of Alkaline Earth Metal Ions with Carboxylic Acids in Aqueous Solutions Studied by 13C NMR Spectroscopy, Zeitschrift für Naturforschung A, 53(1-2), 77-91.
26. Konkena B., S. Vasudevan (2012). Understanding Aqueous Dispersibility of Graphene Oxide and Reduced Graphene Oxide through pKa Measurements, J Phys Chem Lett, 3(7), 867-872.
27. Krishna G., T. Shutava, Y. Lvov (2005). Lipid Modified Polyelectrolyte Microcapsules with Controlled Diffusion, Chem Commun, 22, 2796-2798.
28. Kurapati R., A. M. Raichur (2012). Graphene Oxide Based Multilayer Capsules with Unique Permeability Properties: Facile Encapsulation of Multiple Drugs, Chem Commun, 48(48), 6013-6015.
29. Loretta L. D. M., F. Guerra, G. Lazzari, C. Nobile, et al. (2016). Biocompatible Multilayer Capsules Engineered with a Graphene Oxide Derivative: Synthesis, Characterization and Cellular Uptake, Nanoscale, 8(14), 7501-7512.
30. Manna U., S. Patil (2009). Dual Drug Deliveri Microcapsules via Layer-by-layer Self-assembly, Langmuir, 25(18), 10515-10522.
31. Mendelsohn J. D., C. J. Barrett, V. V. Chan, A. J. Pal, et al. (2000). Fabrication of Microporous Thin Films from Polyelectrolyte Multilayers, Langmuir, 16(11), 5017-5023.
32. Moghimi S. M., P. Symonds, J. C. Murray, A. C. Hunter, et al. (2005). A Two-stage Poly(ethylenimine)-mediated Cytotoxicity: Implications for Gene Transfer, Therapy, 11(6), 990-995.
33. Muthana A., T. M. McCoy, I. R. McKinnon, M. Majumder, R. F. Tabor (2017). Synthesis and Characterization of Graphene Oxide-polystyrene Composite Capsules with Aqueous Cargo via a Water-oil-water Multiple Emulsion Templating Route, ACS Appl Mater Interfaces, 9(21), 18187-18198.
34. Østberg T., C. Graffner (1994). Calcium Alginate Matrices for Oral Multiple Unit Administration: III. Influence of Calcium Concentration, Amount of Drug Added and Alginate Characteristics on Drug Release, Int J Pharm, 111(3), 271-282.
35. Petrov A., D. V. Volodkin, G. B. Sukhorukov (2005). Protein-calcium Carbonate Coprecipitation: A Tool Protein Engapsulation, Biotechnol Prog, 21(3), 918-925.
36. Qi W., Z. Xue, W. Yuan, H. Wang (2014). Layer-by-layer Assembled Graphene Oxide Composite Films for Enhanced Mechanical Properties and Fibroblast Cell Affinity, Journal of Materials Chemistry B, 2, 325-331.

37. Ribeiro C., J. Borges, A. M. S. Costa, V. M. Gaspar, et al. (2018). Preparation of Well-dispersed Chitosan/Alginate Hollow Multilayered Microcapsules for Enhanced Cellular Internalization, Molecules, 23(3), 625.
38. Rodrigues S., M. Dionisio, C. R. Lopez, A. Grehna (2012). Biocompatibility of Chitosan Carriers with Application in Drug Delivery, J Funct Biomater, 3(3), 615-641.
39. Russo R., M. Malinconico, G. Santagata (2007). Effect of Cross-linking with Calcium Ions on the Physical Properties of Alginate Films, Biomacromolecules, 8(10), 3193-3197.
40. Silva C. M., F. Veiga, A. J. Ribeiro, N. Zerrouk, P. Arnaud (2006). Effect of Chitosan-Coated Alginate Microspheres on the Permeability of Caco 2 Cell Monolayers, Drug Dev Ind Pharm, 32(9), 1079-1088.
41. Spielmann H., M. Balls, J. Dupius, W. J. W. Pape, et al. (1998), The International EU/COL-IPA *in vitro* Phototoxicity Validation Study: Results of Phase II (Blind Trial). Part 1: The 3T3 NRU Phototoxicity Test, Toxicology *in vitro*, 305-327.
42. Städler B., A. D. Price, A. N. Zelikin (2001). A Critical Look at Multilayered Polymer Capsules in Biomedicine: Drug Carriers, Artificial Organelles, and Cell Mimics, Adv Funct Mater, 21(1), 14-28.
43. Suk J. W., R. Piner, J. An, R. Ruoff (2010). Mechanical Properties of Monolayer Graphene Oxide, ACS Nano, 4, 6557-6564.
44. Sukhorukov G. B., H. Möhwald (2007). Multifunctional Cargo Systems for Biotechnology, Trends Biotechnol, 25(3), 93-98.
45. Sun H., E. Wong, Y. Yan, J. Cui, et al. (2015). The Role of Capsule Stiffness on Cellular Processing, Chem Sci, 6(6), 3505-3514.
46. Teo G. H., Y. H. Ng, P. B. Zetterlund, S. C. Thickett (2015). Factors Influencing the Preparation of Hollow Polymer-graphene Oxide Microcapsules via Pickering Miniemulsion Polymerization, Polymer, 63, 1-9.
47. Volodkin D. V., A. I. Petrov, M. Prevot, G. B. Sukhorukov (2004). Matrix Polyelectrolyte Microcapsules: New System for Macromolecule Encapsulation, Langmuir, 20(8), 3398-3406.
48. Volodkin D. V., N. I. Larionova, G. B. Sukhorukov (2004). Protein Encapsulation via Porous $CaCO_3$ Microparticles Templating, Biomacromolecules, 5(5), 1962-1972.
49. Wagner E., J. Kloeckner (2005). Gene Delivery Using Polymer Therapeutics, In: Polymer Therapeutics I. Advances in Polymer Science, Satchi-Fainaro R., R. Duncan (Eds.), Vol. 192, Springer, Berlin, Heidelberg, 135-173.
50. Wang M., Y. Niu, J. Zhou, H. Wen, et al. (2016). The Dispersion and Aggregation of Graphene Oxide in Aqueous Media, Nanoscale, 8(30), 14587-14592.
51. Williams D. F. (1987). Definitions of Biomaterials. Progress in Biomedical Engineering 4, Proceedings of a Consensus Conference of the European Society for Materials, Chester, UK, Elsevier, Amsterdam, 72 pp.
52. Yi X., H. Gao (2015). Cell Membrane Wrapping of a Spherical Thin Elastic Shell, Soft Matter, 11(6), 1107-1115.
53. Zhihua A., K. Kavanoor, M. L. Choy, L. J. Kaufman (2009). Polyelectrolyte Microcapsule Interactions with Cells in Two- and Three-dimensional Culture, Colloids Surf B Biointerfaces, 70(1), 114-123.
54. Zin F. A. M., A. M. Noor, W. N. W. M. Nasri, N. N. Roslan, et al. (2020). Synthesis of Sodium Alginate Graphene Oxide-silver Film for Antibacterial Activity, IOP Conference, Ser.: Earth Environ Sci, 596, 012041.

Senior Res. Assist. Svetozar Stoichev, Ph.D.
E-mail: sd_stoichev@abv.bg

Svetozar Stoichev works in the Institute of Biophysics and Biomedical Engineering, Bulgarian Academy of Sciences (BAS) since 2009 and obtained his Ph.D. Degree in Biophysics in 2015. He has already gained experience in preparation of thin polymer coatings and in characterization of surface properties and biocompatibility of coatings composed of hyaluronic acid and chitosan, in the presence or absence of graphene oxide. He has specialized in a month at the Institute of Natural and Medical Sciences at the University of Tübingen, Germany, on a research project to optimize polyelectrolyte multilayer coatings for the biofunctionalization of coronary stents.

Senior Res. Assist. Avgustina Danailova, Ph.D.
E-mail: avgustina_danailova@abv.bg

Avgustina Danailova obtained her Ph.D. Degree in Biophysics in 2021. Currently she is working in the Institute of Biophysics and Biomedical Engineering, BAS and Faculty of Medicine, Sofia University "St. Kliment Ohridski". Her area of research interest includes biofunctionalization of surfaces with polyelectrolyte multilayers for medical products, such as cardiovascular stents, microcarriers of medicinal substances, calorimetric markers for diagnosis and monitoring of diseases.

Assoc. Prof. Ivan Iliev, Ph.D.
E-mail: taparsky@abv.bg

Ivan Iliev is an Associate Professor at the Institute of Experimental Morphology, Pathology and Anthropology with Museum, BAS, where he received Ph.D. Degree in the area of Immunology. His interests are in the field of immunology, biochemistry and cell biology.

Inna Sulikovska, M.Sc.
E-mail: inna_sulikovska@ukr.net

Inna Sulikovska works at the Institute of Experimental Morphology, Pathology and Anthropology with Museum, BAS. She received M.Sc. Degree in the area of Biomedical Engineering at the National Technical University of Ukraine "Igor Sikorskyi Kyiv Polytechnic Institute". Her areas of interests are in the field of biomedical engineering, nanomaterials, stem cells differentiation, pathology, cancer cell biology.

Senior Res. Assist. Velichka Strijkova, Ph.D.
E-mail: vily_strij@abv.bg

Velichka Strijkova works in the Institute of Optical Materials and Technologies "Acad. Jordan Malinovski", BAS since 1999 and in the Institute of Biophysics and Biomedical Engineering, BAS since 2018. She defended Ph.D. Degree in Physical Chemistry in the Institute of Optical Materials and Technologies, BAS in 2014. She has experience in various research areas such as polyimide films, vacuum deposited thin layers, nanocomposite materials and nanotechnology, organic solar cells, atomic force microscope (AFM) – Full complement of operating modes for fluid and air operation, including: Contact/Lateral Force, non-contact AC mode, Intermitten-contact mode, electric force microscopy, conductive c-AFM, force spectroscopy and force volume, I-V spectroscopy.

Senior Res. Assist. Kirilka Mladenova, Ph.D.
E-mail: keti.mladenova@abv.bg

Kirilka Mladenova is Senior Research Assistant in the Department of Biochemistry, Sofia University "St. Kliment Ohridski", since 2017. She obtained her B.Sc. Degree on Molecular biology in 2011, M.Sc. Degree on Cell biology and Pathology in 2013 and Ph.D. degree on Molecular Biology in 2017. The research area of her present work includes cell polarity, protein sorting and targeting, lipid rafts, signal transduction, retinal dystrophies, lipid-protein interactions, model membrane systems and testing of biologically active agents on cell lines. She is laureate of L'Oréal-UNESCO "For Women in Science" program in Bulgaria for 2017.

Assoc. Prof. Tonya Andreeva, Ph.D.
E-mail: t_andreeva@abv.bg

Tonya Andreeva is an Associate Professor at the Institute of Biophysics and Biomedical Engineering, BAS. She has got her Ph.D. Degree in Biophysics in the same Institute at 2006 with a thesis focused on the model lipid membranes with controllable morphology and surface potential. She has published more than 30 research articles in the area of biophysics, plant science, physical chemistry, polymer science, and biomedicine. She participated on more than 50 national and international conferences and in 20 scientific projects in collaboration with numerous national and international institutes and universities.